

Stroke patterns and regulation of swim speed and energy cost in free-ranging Brünnich's guillemots

James R. Lovvorn^{1,*}, Yutaka Watanuki², Akiko Kato³, Yasuhiko Naito³ and Geoffrey A. Liggins^{4,†}

¹Department of Zoology, University of Wyoming, Laramie, WY 82071, USA, ²Graduate School of Fisheries Sciences, Hokkaido University, Minato-cho 3-1-1, Hakodate 041-8611, Japan, ³National Institute of Polar Research, 9-10 Kaga 1-chome, Itabashi-ku, Tokyo 173-8515, Japan and ⁴Department of Mechanical Engineering, University of British Columbia, Vancouver, BC V6T 1Z4, Canada

*Author for correspondence (e-mail: lovorn@uwyo.edu)

†Present address: C-CORE, Memorial University of Newfoundland, St John's, NF A1B 3X5, Canada

Accepted 4 October 2004

Summary

Loggers were attached to free-ranging Brünnich's guillemots *Uria lomvia* during dives, to measure swim speeds, body angles, stroke rates, stroke and glide durations, and acceleration patterns within strokes, and the data were used to model the mechanical costs of propelling the body fuselage (head and trunk excluding wings). During vertical dives to 102–135 m, guillemots regulated their speed during descent and much of ascent to about $1.6 \pm 0.2 \text{ m s}^{-1}$. Stroke rate declined very gradually with depth, with little or no gliding between strokes. Entire strokes from 2 m to 20 m depth had similar forward thrust on upstroke vs downstroke, whereas at deeper depths and during horizontal swimming there was much greater thrust on the downstroke. Despite this distinct transition, these differences had small effect (<6%) on our estimates of mechanical cost to propel the body fuselage, which did not include drag of the wings. Work stroke⁻¹ was quite high as speed increased dramatically in the first 5 m of descent against high buoyancy. Thereafter, speed and associated drag increased gradually as buoyancy slowly declined, so that mechanical work stroke⁻¹ during the rest of descent stayed

relatively constant. Similar work stroke⁻¹ was maintained during non-pursuit swimming at the bottom, and during powered ascent to the depth of neutral buoyancy (about 71 m). Even with adjustments in respiratory air volume of $\pm 60\%$, modeled work against buoyancy was important mainly in the top 15 m of descent, after which almost all work was against drag. Drag was in fact underestimated, as our values did not include enhancement of drag by altered flow around active swimmers. With increasing buoyancy during ascent above 71 m, stroke rate, glide periods, stroke acceleration patterns, body angle and work stroke⁻¹ were far more variable than during descent; however, mean speed remained fairly constant until buoyancy increased rapidly near the surface. For dives to depths >20 m, drag is by far the main component of mechanical work for these diving birds, and speed may be regulated to keep work against drag within a relatively narrow range.

Key words: bird swimming, buoyancy, costs of diving, diving birds, drag, guillemots, stroke patterns, swim speed.

Introduction

Because of its key influence on locomotor cost and efficiency, swim speed is an important element in foraging models for marine endotherms (Wilson, 1991; Houston and Carbone, 1992; Thompson et al., 1993; Boyd et al., 1995; Wilson et al., 1996; Grémillet et al., 1998a, 1999; Lovvorn et al., 1999; Hindell et al., 2000). It is often found that birds and mammals swim underwater at or near the speed of minimum cost of transport (COT, $\text{J kg}^{-1} \text{ m}^{-1}$) (Ponganis et al., 1990; Culik et al., 1991; Williams et al., 1993; Ropert-Coudert et al., 2001). However, it is difficult to predict the speed of minimum COT throughout dives, because important factors that affect energy costs of diving change with depth and phase of the dive (descent, ascent, and horizontal swimming at the main depth of foraging).

For example, because air volumes in the respiratory system and plumage change with hydrostatic pressure, work against buoyancy varies dramatically with depth (Lovvorn and Jones, 1991a; Wilson et al., 1992; Lovvorn et al., 1999; Skrovan et al., 1999). It has been suggested that penguins, cormorants and sea turtles manipulate their air volumes or dive depths to optimize the effects of buoyancy on dive costs (Hustler, 1992; Minamikawa et al., 2000; Sato et al., 2002; Hays et al., 2004). However, as the thickness of the insulative layer of air in bird plumage is compressed with increasing depth, heat loss increases (Grémillet et al., 1998b), perhaps creating a conflict between decreased work against buoyancy and increased costs of thermoregulation. Work against buoyancy becomes minimal

below the depth at which most compression of air spaces has occurred (~20 m; Lovvorn and Jones, 1991a; Lovvorn, 2001), and much of the energy expended against buoyancy during descent may be recovered during ascent (Lovvorn et al., 1999). Thus, the influence of buoyancy manipulation on total cost of a dive will decrease rapidly with increasing dive depth, and may be negligible for deeper dives by many bird species.

Another potential determinant of swim speed is the fact that, for muscles containing mostly similar fiber types such as alcid flight muscles (Kovacs and Meyers, 2000), muscle contraction is most efficient over a relatively narrow range of contraction speeds and loads (Lovvorn et al., 1999, and references therein). Consequently, as buoyant resistance changes with depth, swim speed may be altered to bring about compensatory changes in work against drag, thereby conserving work stroke⁻¹. Alternatively, gliding between strokes may be used to prevent changes in speed as buoyant resistance changes, without altering contraction speed or work stroke⁻¹ (Lovvorn et al., 1999; van Dam et al., 2002; Watanuki et al., 2003). Changes in work during the upstroke with varying forward speed have been identified in aerial flight (Rayner et al., 1986; Hedrick et al., 2002; Spedding et al., 2003), but such patterns have not been investigated in diving birds.

Especially at depths below which buoyancy becomes negligible, simulation models suggest that the main determinant of the mechanical cost of swimming is hydrodynamic drag (Lovvorn, 2001). Based on tow-tank measurements of the drag of a frozen common guillemot (COGU, *Uria aalge*) mounted on a sting, Lovvorn et al. (1999) suggested that the mean speed observed in free-ranging Brünnich's guillemots (BRGU, *Uria lomvia*) was that which minimized the drag coefficient. These authors also predicted that, for reasons of muscle contraction efficiency, mean speed was regulated by altering glide duration while work stroke⁻¹ remained constant. However, the inference about choice of mean speed did not account for effects of accelerational (oscillatory) stroking, in which instantaneous speed varies widely throughout individual strokes.

In subsequent analyses of work against drag and inertia throughout strokes during horizontal swimming (Lovvorn and Liggins, 2002), models suggested that dividing thrust between upstroke and downstroke as in wing-propelled divers, as opposed to having all thrust on the downstroke as in most foot-propelled divers, had important effects on swimming costs. At the same mean speed, higher instantaneous speeds during stronger downstrokes incurred higher drag, owing to the rapid nonlinear increase of drag with increasing speed. However, the stroke–acceleration curves used in those models were only reasonable approximations, having never been directly measured. At that time, the only way to measure such patterns was by high-speed filming (Lovvorn et al., 1991; Johansson and Aldrin, 2002; Johansson, 2003), either during horizontal swimming or during vertical dives in shallow tanks where buoyancy is quite high and strongly influences stroke–acceleration patterns. Subsequent advances in instrumentation have allowed measurement of acceleration throughout strokes

in free-ranging birds. Results indicate that stroke–acceleration patterns of BRGU change with dive depth and among descent, ascent and horizontal swimming (Watanuki et al., 2003). These new instruments provide an opportunity to incorporate complete empirical data into models that include effects of accelerational stroking on work against drag.

When swimming in a horizontal tank 33.5 m long to reach food supplied at the other end, COGU typically swam at speeds of 2.2–2.6 m s⁻¹ (Swennen and Duiven, 1991; see also Bridge, 2004). However, free-ranging BRGU in Canada and Norway regulated their speed throughout descent and ascent within a narrow range of about 1.6±0.2 m s⁻¹, despite large changes in buoyancy with depth (Lovvorn et al., 1999; Watanuki et al., 2003). These birds appeared to be feeding on or near the sea floor or in distinct epipelagic layers (Lovvorn et al., 1999; Mehlum et al., 2001), showing sustained speeds during transit between the surface and relatively stationary food resources.

To investigate the reasons for these speed patterns and ways they are achieved, we used loggers on free-ranging BRGU to describe swim speeds, body angles, stroke rates, stroke and glide durations, and relative thrust on upstroke vs downstroke throughout dives (Watanuki et al., 2003), and used these data in a simulation model of dive costs. In particular, we tested for effects of mean swim speeds and varying stroke–acceleration patterns on dive costs, given the rapid nonlinear increase of drag with increasing speed. We also asked whether work stroke⁻¹ remained relatively constant, while speed was regulated by varying the duration of glide periods between strokes.

Materials and methods

Body mass and surface area, body and air volumes, buoyancy and drag

Various parameters for the birds' bodies were needed for modeling. Individuals fitted with time–depth recorders (TDRs, see below) were weighed upon their return from foraging trips. Body mass M_b was 1.00 kg for BRGU 82, 0.90 kg for BRGU 87 and 0.94 kg for BRGU 13. Wetted surface area A_{sw} (mean ± s.d.) of four BRGU collected in the Bering Sea, USA ($M_b=1.176±0.063$ kg) was 0.0922±0.0047 m² (measured as in Lovvorn et al., 1991). Owing to the large effects of respiratory volume, total body volume V_b is best measured on live birds (Lovvorn and Jones, 1991a,b). For BRGU, V_b (in l) was estimated from a curve based on water displacement of living specimens of a range of duck and seabird species: $V_b=0.0137+1.43M_b$ (Lovvorn and Jones, 1991b).

Volume of air in the respiratory system (in l) was estimated by $V_{resp}=0.1608M_b^{0.91}$ (Lasiewski and Calder, 1971). To assess effects on dive costs of active regulation of respiratory volume by the birds, costs were modeled with respiratory volume at ±60% of the value used in all other simulations (0.153 l); this percentage range corresponds to that estimated for freely diving king penguins (*Aptenodytes patagonicus*) by Sato et al. (2002). Volume of the plumage air layer (V_{plum} , l) of our instrumented birds, estimated by the equation of Lovvorn and

Jones (1991a) based on dead diving ducks *Aythya* spp. ($V_{\text{plum}}=0.2478+0.1232M_b$), yielded a mean of 0.365 l kg^{-1} for the instrumented BRGU. Air volumes calculated here are presumed to be those upon initial submersion at the start of a dive. The buoyancy of air is 9.79 N l^{-1} (Lovvorn et al., 1999). The buoyancy of body tissues, based on water, lipid, protein and ash content of the body, was calculated to be -0.626 N or -0.659 N kg^{-1} for the mean body mass of the instrumented BRGU (0.95 kg ; see Lovvorn et al., 1999).

Hydrodynamic drag D (in N) of single frozen specimens of COGU and BRGU was measured at a range of speeds U (m s^{-1}) in a tow tank. Propulsive limbs (wings only for guillemots) were removed from the body fuselage (head and trunk). Drag of the same COGU was measured both when mounted on a sting (a rod which enters the bird from the rear) (Lovvorn et al., 1999) and when towed by a harness and drogue system (Lovvorn et al., 2001). Drag of the BRGU was measured only with the harness and drogue (Lovvorn et al., 2001). The drag data were also expressed in terms of dimensionless drag coefficients ($C_D=2D/\rho A_{\text{sw}}U^2$) and Reynolds numbers ($Re=UL_b/\nu$), where ρ is the density (1026.9 kg m^{-3}) and ν is the kinematic viscosity ($1.3538 \times 10^{-6} \text{ m}^2 \text{ s}^{-1}$) of salt water at 10°C ; surface areas and body lengths L_b are given in Lovvorn et al. (2001). Dimensionless $C_D:Re$ curves are the same for the same shape regardless of variation in size.

Studies of anguilliform and thunniform swimmers, which propel themselves by flexing the body itself, have shown that actively swimming animals have higher drag than gliding or frozen specimens (Webb, 1971; Williams and Kooyman, 1985; Fish, 1988, 1993). However, these swimming modes are quite different from those of penguins and alcids, which maintain a rather rigid fuselage while stroking with lateral propulsors. During swimming, the wings of guillemots are shaped into a narrow proximal 'strut' separating the body from a distal and broader lift-generating surface (see illustrations in Spring, 1971); such shapes can substantially reduce interference drag caused by interactions of flow around oscillating propulsive limbs and the body fuselage (Blake, 1981). Although even streamlined attachments to the body can cause interference drag (see Tucker, 1990), differences in the fuselage drag of frozen vs swimming animals may be far less for guillemots than for anguilliform swimmers. Such effects are still probably appreciable, but no measurements have been made to allow their estimation for wing-propelled swimmers, and we did not consider them. Drag coefficients determined from the deceleration of gliding alcids were similar to those from our measurements (Johansson, 2003).

Stroke periods, stroke acceleration curves and inertial work

The periods (durations) of wing strokes, and acceleration of the body fuselage throughout entire strokes (including both upstroke and downstroke), were determined from accelerometer data. Based on acceleration parallel to the body fuselage (surge) recorded at 0.03125 s intervals (32 Hz), plots of acceleration throughout each stroke were used to distinguish the beginning and end of each stroke. Plots of each stroke were

superimposed to identify groups of strokes with similar periods and acceleration patterns. Data from groups of similar strokes were then fitted with stepwise multiple regression. The shapes of the fuselage acceleration curves were complex, and we wished to fit them closely to capture important aspects of these shapes. Consequently, we selected models from combinations of up to 12 polynomial terms, and visually examined plots to arrive at the simplest model that closely fit the data (see Lovvorn et al., 2001).

For groups of strokes with similar acceleration curves, we then calculated changes in fuselage speed at 0.03125 s intervals throughout strokes, starting with the mean speed at that depth estimated from the TDR data, and the appropriate acceleration curve for that depth. We averaged these calculated speeds at the end of each interval, and determined the difference between this average and the estimated mean speed (from the TDR) at the end of the stroke. This difference was then added (or subtracted) to the speed at the end of each interval, so that the new average over all intervals resulted in no change in mean speed during the stroke. We then expressed the speed at the end of each interval as the fraction of mean stroke speed vs fraction of stroke period, so that curves fitted to these values could be applied to different mean speeds throughout a dive. These curves did not include much smaller values of net acceleration over the entire stroke needed to achieve observed small increments in overall mean speed. Resulting curves were fitted with stepwise multiple regression to yield polynomials used in the model.

Water displaced from in front of a swimming animal must be accelerated around the animal to fill the space vacated behind it. Added mass is the mass of that accelerated water, and the added mass coefficient α is the ratio of the added volume of water to body volume (Daniel, 1984; Denny, 1988). For ideal fluids with no viscosity, plots have been developed that relate α to ratios of the three axes of an ellipsoid that describe the object (Kochin et al., 1964). Based on total body length minus length of the culmen, and maximum height and width of the body, we used these plots to estimate α for BRGU as 0.075 (Lovvorn and Liggins, 2002). Added mass was calculated as $M_a=\alpha\rho V_b$, where ρ is the density of salt water at 10°C (1026.9 kg m^{-3}) and V_b is total body volume (see above). The force G (in N) required to accelerate the virtual mass (M_b+M_a), known as the acceleration reaction (Denny, 1988), was calculated as $G=-(M_b+M_a)(dU/dt)$, where dU/dt is the change in speed over intervals of 0.02 s .

In real fluids such as water that have viscosity, some of the momentum imparted to the added mass may be dissipated in the fluid during the stroke. Vortices shed from the entrained boundary layer may move away from the body, thereby decreasing the added mass (Sarpkaya and Isaacson, 1981). In this way, part of the forward-directed, in-line work done by the animal to accelerate the added mass during the power phase of the stroke can be lost in the free stream, thereby decreasing the momentum remaining to propel the body forward passively during deceleration in the recovery phase. Although loss of momentum in a shed vortex imparts an opposite impulse on

the bird's body, this opposing impulse would typically not be in line with the direction of swimming. This loss of momentum *via* shedding of added mass means that the animal may do net positive inertial work over the entire stroke cycle, when there is no net acceleration of the body in line with the direction of motion over that stroke cycle.

Unfortunately, for real fluids there is no theory for estimating added mass and its variations, which are affected in complex ways by the shape and surface roughness of the object, and the pattern of acceleration. The only measurements have been for simple motions and shapes such as oscillating cylinders (Sarpkaya and Isaacson, 1981). Nevertheless, these measurements indicate that added mass during the acceleration phase can be much higher than during deceleration, so that the force exerted on the fluid by the cylinder during acceleration is less than the in-line, forward force exerted on the cylinder by the fluid during deceleration. This effect is presumed to result from vortex shedding of added mass between acceleration and deceleration phases (Sarpkaya and Isaacson, 1981).

This mechanism may explain why calculations based on instantaneous velocities measured from high-speed films have indicated positive inertial work over entire stroke cycles in animals swimming by oscillatory strokes without net acceleration along the direction of motion (Gal and Blake, 1988; Lovvorn et al., 1991; Lovvorn, 2001). Thus, the frequent assertion that the acceleration reaction must sum to zero over entire stroke cycles when mean speed is constant (e.g. Stephenson, 1994), which may be true for inviscid fluids (Batchelor, 1967; Daniel, 1984), is not necessarily true for real fluids. In fact, in viscous fluids where some dissipation of momentum is unavoidable, analyses of oscillatory stroking at constant mean speed that do not account for inertial work may be incomplete.

If the added mass coefficient changes throughout strokes, and there are no theories or measurements for estimating added mass in real fluids, what value of α should be used? We used the value for ideal fluids described above as a constant for the entire stroke cycle. This convention probably causes overestimates of negative inertial work during the recovery phase, so our resulting values of net inertial work may be conservative. Some of the same boundary-layer and vortex dynamics that alter the drag coefficient with changes in speed also change the added mass coefficient, so drag and added mass effects are probably not independent. However, we make the conventional assumption that work against drag and inertia are additive (Morison et al., 1950). This assumption has been the subject of much research, but no better operational approach has yet been developed (Denny, 1998; review in Sarpkaya and Isaacson, 1981).

Calculation of work throughout strokes

Work throughout swimming strokes was modeled by calculating the linear distance moved by the body fuselage (head and trunk without propulsive limbs) during 0.02 s intervals, according to the equations relating fraction of mean

stroke speed to fraction of stroke period. Inertial (accelerational) work was the work done to accelerate the body and the added mass of entrained water over each 0.02 s interval. Work against drag and buoyancy (W_{D+B}) was calculated by multiplying drag (D) and buoyancy (B) at the given depth by displacement during the same time interval (ds/dt): $W_{D+B}=(D+B)(ds/dt)$. Body angle was considered in calculating vertical work against buoyancy. We used a quasi-steady modeling approach, in which drag of the body fuselage for a given interval during the stroke is assumed to be the same as drag at that speed under steady conditions. In quasi-steady fashion, work to overcome drag, buoyancy and inertia during each 0.02 s interval was then integrated over the entire stroke to yield total work parallel to the body fuselage during the stroke (Lovvorn et al., 1991, 1999). This calculation of work for forward swimming does not include work perpendicular to the body (heave), or of any pitching or yawing movements.

Our estimates of mechanical costs were for propelling the body fuselage, and did not include models of the complex flows around oscillating propulsive limbs (e.g. Spedding et al., 2003). The reduced frequency parameter has been used to judge when quasi-steady *vs* unsteady models for propulsive limbs are justified (Spedding, 1992; Dickinson, 1996). Alcid wings exhibit time-variable shape and movement, being swept back and flexing at the wrist and stationary where attached to the body (Johansson and Aldrin, 2002; Johansson, 2003). These aspects make it difficult to determine the effective chord length (blade width) needed to calculate the reduced frequency (but see Johansson, 2003), or at least argue for separate consideration of different wing segments (Hedrick et al., 2002). Work on unsteady (*vs* quasi-steady) flow around oscillating propulsors has focused on rigid robotic limbs with constant planform (e.g. Dickinson, 1996; Dickinson et al., 1999), and only recently has the more complex situation of flexing wings with varying shape been explored (Combes and Daniel, 2001; Hedrick et al., 2002). Consequently, when our models are used to estimate food requirements (e.g. Lovvorn and Gillingham, 1996), the efficiency of propulsive limbs is subsumed in an aerobic efficiency (mechanical power output \div aerobic power input) by which the limbs propel the body fuselage. For this paper, however, our intent is to evaluate the mechanical cost of propelling the body fuselage at speeds and accelerations measured with loggers throughout swimming strokes, and values of mechanical work have not been adjusted by an aerobic efficiency.

Time-depth recordings and accelerometry

Electronic TDRs were attached to wild birds captured on their nests (Watanuki et al., 2003). Recorders measured depth (pressure) with accuracy of 1 m and resolution of 0.1 m. Near Ny-Ålesund, Svalbard, Norway in July 1998 (76–81°N, 20–25°E; see Mehlum and Gabrielsen, 1993; Mehlum et al., 2001), nine BRGU (including numbers 82 and 87) were fitted with TDRs (15 mm wide \times 48 mm long, 14 g, Little Leonardo Ltd., Tokyo) that recorded depth every 1 s (Watanuki et al., 2001). Also near Ny-Ålesund in July 2001, three BRGU

(including number 13) were fitted with loggers that recorded depth at 1 Hz and acceleration at 32 Hz (2-axis capacitive sensor, ADXL202E, Analog Devices, Norwood, MA, USA). The latter packages could measure both dynamic acceleration (as by propulsion) and static acceleration (such as gravity), allowing calculation of body angle based on the low-frequency component of surge acceleration (Sato et al., 2002; Watanuki et al., 2003). The angle between the logger and the axis of the bird's body was determined by assuming that the bird's body axis was horizontal when the bird was floating on the water surface; there may have been a small difference between this body axis and that during underwater swimming. Body angle during dives was corrected for the attachment angle of the logger relative to the body axis of the floating bird. Knowing body angle then allowed calculation of actual swim speed from vertical speed. These loggers were 15 mm × 60 mm, and weighed 16 g (<2% of the birds' mass). The accelerometers measured both tail-to-head (surge) and dorsal-to-ventral (heave) accelerations; for analyses in this paper, only surge data were used. All loggers were attached to feathers on the lower backs of the birds with quick-set glue and cable ties, and were retrieved after one or more foraging trips.

We later selected the deepest dives for calculating dive profiles and vertical speeds. We considered deep dives more likely to reflect sustained descent and ascent without other activities in the water column, so that swimming speeds would correspond either to direct transit to a known prey concentration at a given depth, or searching for prey without immediate pursuit (see Wilson et al., 1996, 2002; Ropert-Coudert et al., 2000). Dives analyzed for BRGU were to depths of 102–135 m; adults collected at sea in this area had eaten mostly epipelagic squids, amphipods, euphausiids and copepods, but chicks were fed demersal polar cod *Boreogadus saida* (Mehlum and Gabrielsen, 1993). The latter pattern resembled that for BRGU in the eastern Canadian arctic, where adults appeared to make many shallower dives to feed themselves on epipelagic prey before making a series of much deeper dives to capture demersal fish for chicks (see Lovvorn et al., 1999).

Results

Drag vs speed in frozen guillemots

Plots of drag vs speed for frozen COGU and BRGU towed by a harness and drogue system were very similar, but were somewhat higher at low speeds than for the same COGU mounted on a sting (Fig. 1A). The latter difference resulted in different curves of C_D vs Re for harness and sting measurements on the same frozen bird, with sting measurements showing appreciably lower Reynolds numbers (Re) at which drag coefficient (C_D) was minimized (Fig. 1B). This difference probably resulted from greater stability of the sting-mounted specimen at low speeds, but inability of the sting to adjust automatically to the angle of minimum drag at high speeds, as was possible with the harness and drogue (Lovvorn et al., 2001). Because effects of drag are greater at

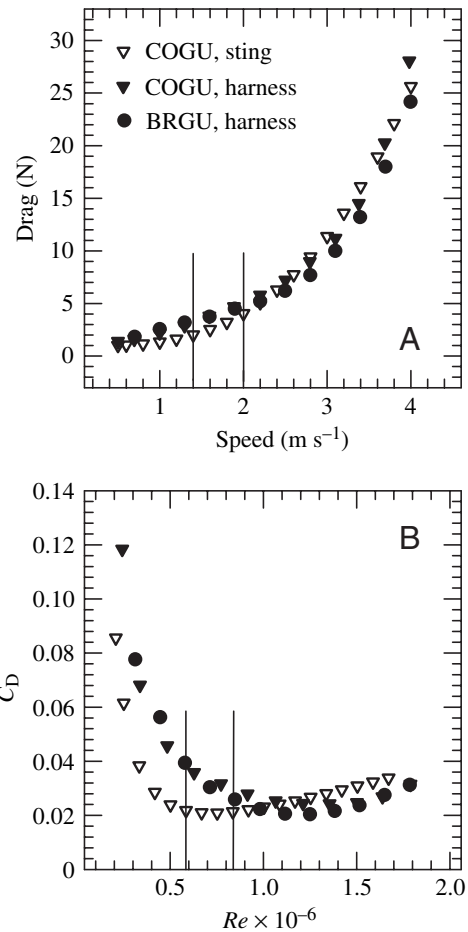


Fig. 1. Fitted curves for (A) drag D (in Newtons) vs speed U (m s^{-1}), and (B) drag coefficient C_D vs Reynolds number Re , measured on frozen birds in a tow tank for a common guillemot (COGU) mounted on a sting (from Lovvorn et al., 1999), and for the same COGU and a Brünnich's guillemot (BRGU) towed with a harness and drogue system (from Lovvorn et al., 2001). Vertical lines indicate the range of speeds and Re observed in free-ranging BRGU during descent and ascent (Figs 2 and 3). The equation for the BRGU towed with the harness and drogue is $D=1.08+2.55U^2-1.38U^3+0.276U^4$.

higher speeds, we used harness and drogue measurements for the BRGU in subsequent calculations.

Consistency of dive patterns in guillemots

As measured with TDRs, patterns of change in depth and vertical speed were very consistent within and between individual BRGU (Fig. 2). Dives shown in Fig. 2 were the deepest dives by these individuals during single foraging trips; they were 'bounce' dives, with little time spent at the bottom. Shallower dives and 'U-shaped' dives with more time spent at the bottom followed similar patterns during descent and ascent. In all cases, vertical speed (vs actual swim speed) during descent increased rapidly in the first 10 m to 1.3–1.4 m s^{-1} , and then increased gradually to 1.7–2.0 m s^{-1} . During ascent, vertical speed again increased over the first 10 m to 1.4–1.6 m s^{-1} , and then increased gradually to about 1.5–1.7 m s^{-1} .

A 'U-shaped' dive to a maximum depth of 113 m by a third individual guillemot with a logger that was 25% longer showed similar rates of depth change during descent and ascent (cf. Figs 2 and 3). During descent, vertical speeds and actual swim speeds were almost identical over a range of mostly 1.5–1.8 m s⁻¹, reflecting the nearly vertical body angle of -80° to -90°. Swim speed increased very rapidly in the first few meters, and increased gradually thereafter from 1.3 to 1.8 m s⁻¹. Body angle and speed varied little above a depth of 90 m. However, in the last 5 m of descent, body angle decreased sharply, thereby reducing vertical speed by about 0.3 m s⁻¹ while swim speed was reduced by only 0.1 m s⁻¹.

During ascent, body angle was very constant to about 63 m, being less vertical (70° from horizontal) than during descent but still steep enough so that vertical speed was only 0.1 m s⁻¹ lower than actual swim speed. Shallower than 63 m, body angle varied over a range of about 17°, resulting in up to 0.8 m s⁻¹ difference between vertical speed and actual swim speed. As during descent, speed increased very rapidly within the first few meters of ascent, ranging thereafter from about 1.3 to 1.6 m s⁻¹. Both vertical and actual swim speeds increased by about 0.7 m s⁻¹ in the last 15–20 m of ascent, when buoyancy rapidly increased.

Given the large changes in buoyant resistance during dives (Fig. 3A), and that very similar COGU can readily swim at speeds of 2.2–2.6 m s⁻¹ (Swennen and Duiven, 1991), the narrow range of speeds during steady descent (mostly 1.6–1.9 m s⁻¹) and the majority of ascent (mostly 1.4–1.7 m s⁻¹) is striking. Variations of only about ±0.2 m s⁻¹ during descent, and during ascent up to depths of ~20 m above which buoyancy rapidly increases, suggest consistent regulation of swim speed. In BRGUs 82 and 87 (Fig. 2), vertical swim speed was about 0.2 m s⁻¹ lower during ascent than descent, perhaps due mostly to differences in body angles (Fig. 3). However, in BRGU 13, actual swim speed during ascent was about 0.3 m s⁻¹ lower than during descent.

Stroke rate of the wings varied little and decreased only slightly with depth during descent. During ascent, stroke rate was far more variable, decreasing up to near the depth of neutral buoyancy (~71 m) but with no obvious trend from there to the surface (Fig. 3).

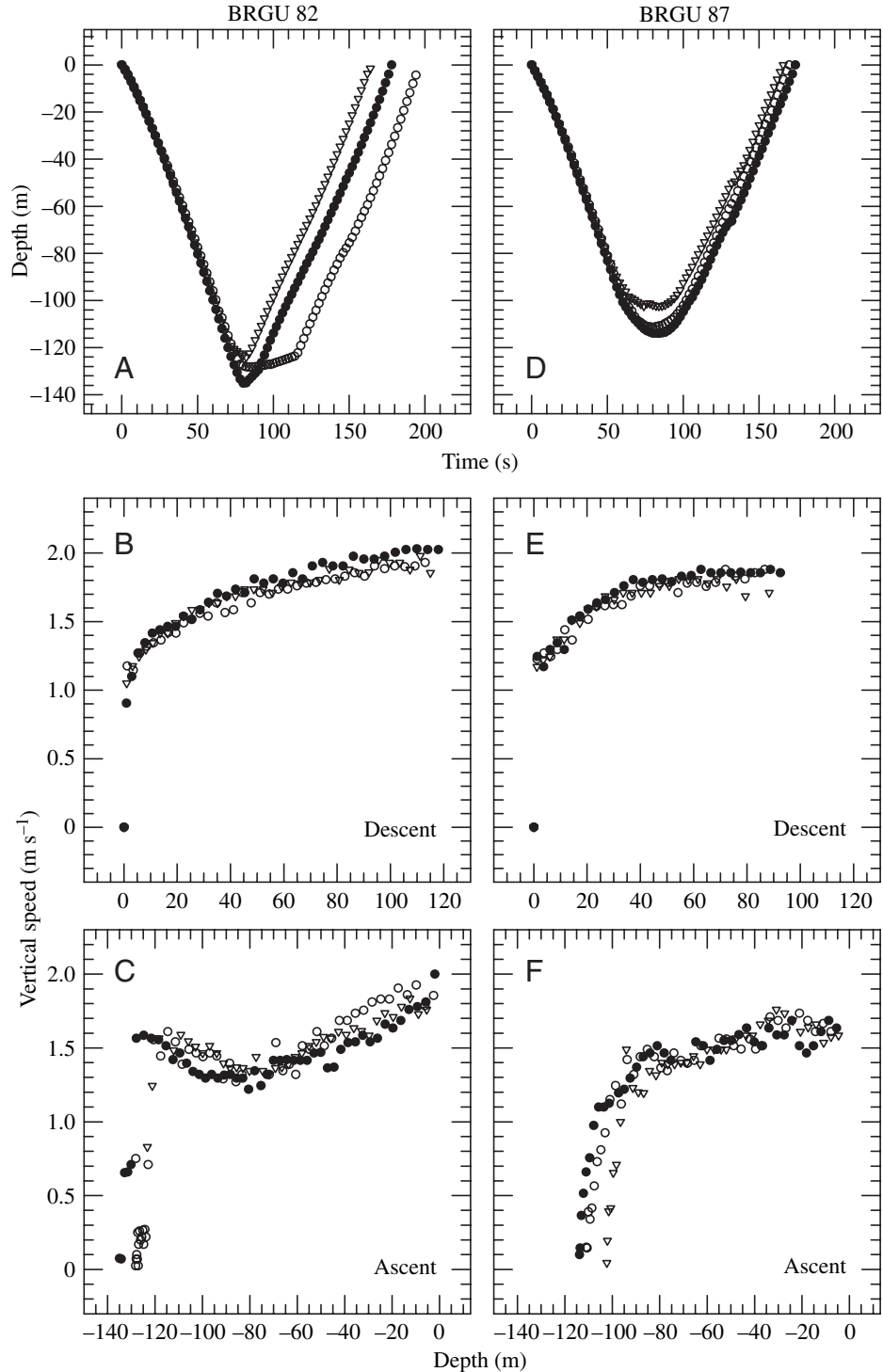


Fig. 2. Changes in depth over time (A,D), and of vertical speed vs depth during descent (B,E) and ascent (C,F), as measured with time-depth recorders (TDRs) during three dives each by two Brunnich's guillemots (A–C; BRGU 82 and D–F; BRGU 87) near Svalbard, Norway. Curves are based on recordings at 1 s intervals.

Acceleration and speed during strokes

Patterns of surge acceleration during swimming strokes changed appreciably with depth during descent and ascent, and between descent, ascent and horizontal swimming (Figs 4, 5). During descent, the first two strokes to a depth of 2 m were quite different from all subsequent strokes, lasting far longer and exhibiting much lower (first stroke) or much higher (second stroke) variation in acceleration during the stroke (Fig. 4A). These two curves include acceleration from a standing start at the water surface against very high buoyancy at the start of the dive. They also encompass a rapid change in body angle from horizontal to vertical, perhaps confounding estimates of work based on measurements of surge acceleration only. For this reason, the first two strokes were not included in calculations of dive cost.

During descent from 2 to 20 m where buoyancy was appreciable (Fig. 3A), relative acceleration during upstroke and downstroke were similar (Fig. 4B). However, deeper than 20 m, where buoyancy was low and changed little with depth, relative acceleration during the upstroke decreased dramatically, and continued a gradual decline to the final stroke of steady descent at 109 m (Fig. 4C; cf. Fig. 3). Relative surge acceleration during the upstroke was even lower during horizontal swimming in the bottom phase of the dive (Fig. 4D). Thus, relative upstroke thrust declined as resistance from buoyancy decreased from shallow descent to deeper descent to horizontal swimming. Stroke frequency declined very slowly with increasing depth during descent (Fig. 3E). Short glide periods, during which speed decreased steadily and very gradually, were difficult to identify from accelerometer data at 0.03125 s intervals (32 Hz). However, it appeared that, during descent, a glide period of about 0.03 s was added to most strokes starting at about 45 m, and that glides were extended to 0.06 s at about 85 m. Because these glides were only 7–13% of stroke period, were variable in occurrence, and were difficult to distinguish, gliding did not appear to be an important component of locomotion during descent in BRGU and was not considered in calculations.

Despite regular trends of change in acceleration patterns during descent and at the bottom, trends during ascent were less consistent. Throughout ascent, surge acceleration was mainly during the downstroke

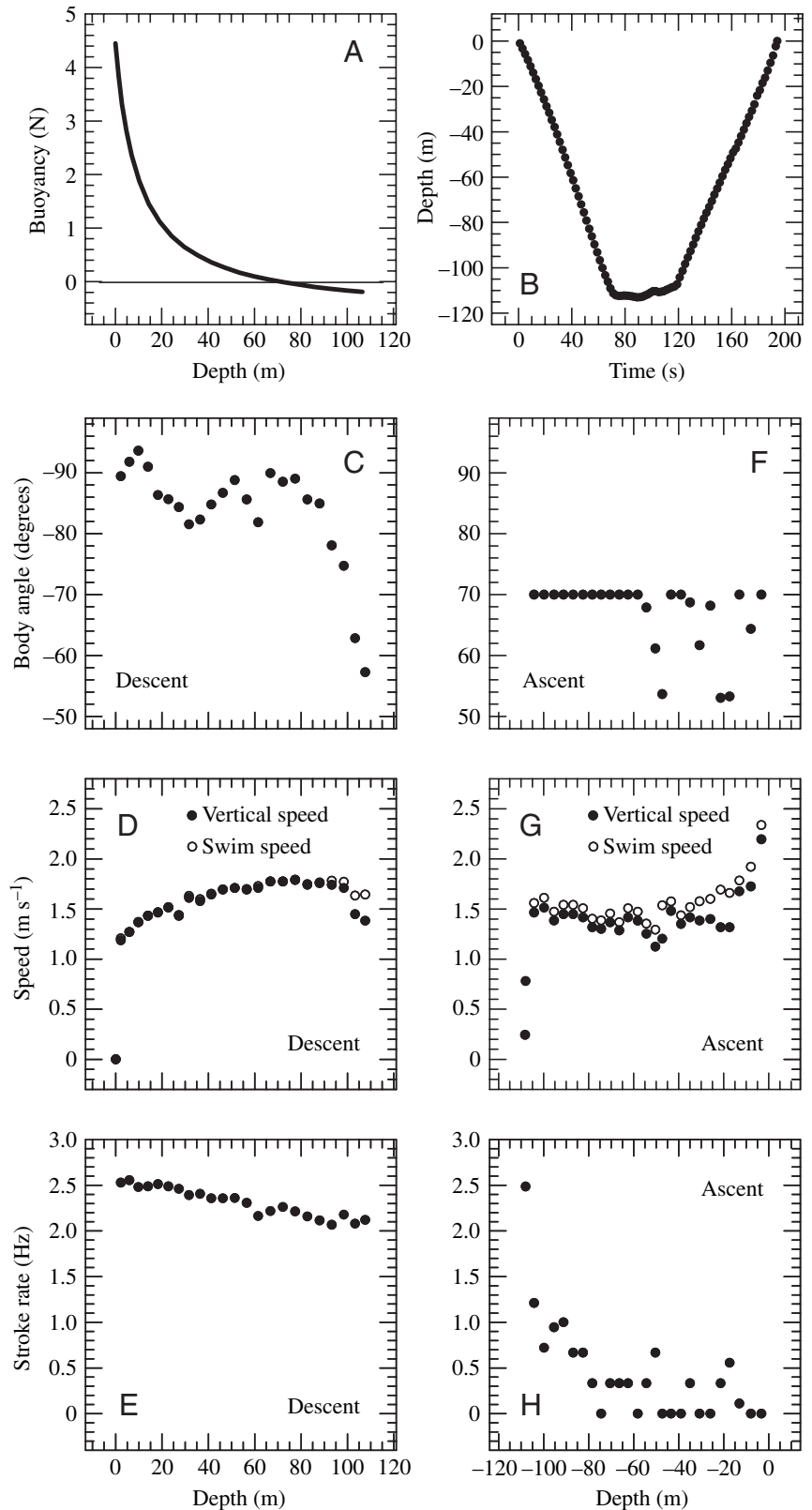


Fig. 3. Changes in (A) estimated buoyancy vs depth and (B) depth vs time, and (C–H) body angle (from horizontal), vertical speed, actual swim speed and stroke rate vs depth, for a Brünnich's guillemot (BRGU 13) during descent to 113 m (C–E) and during ascent (F–H). Values are averages over 3 s intervals of recordings at 1 Hz. The depth of neutral buoyancy was estimated as 71 m.

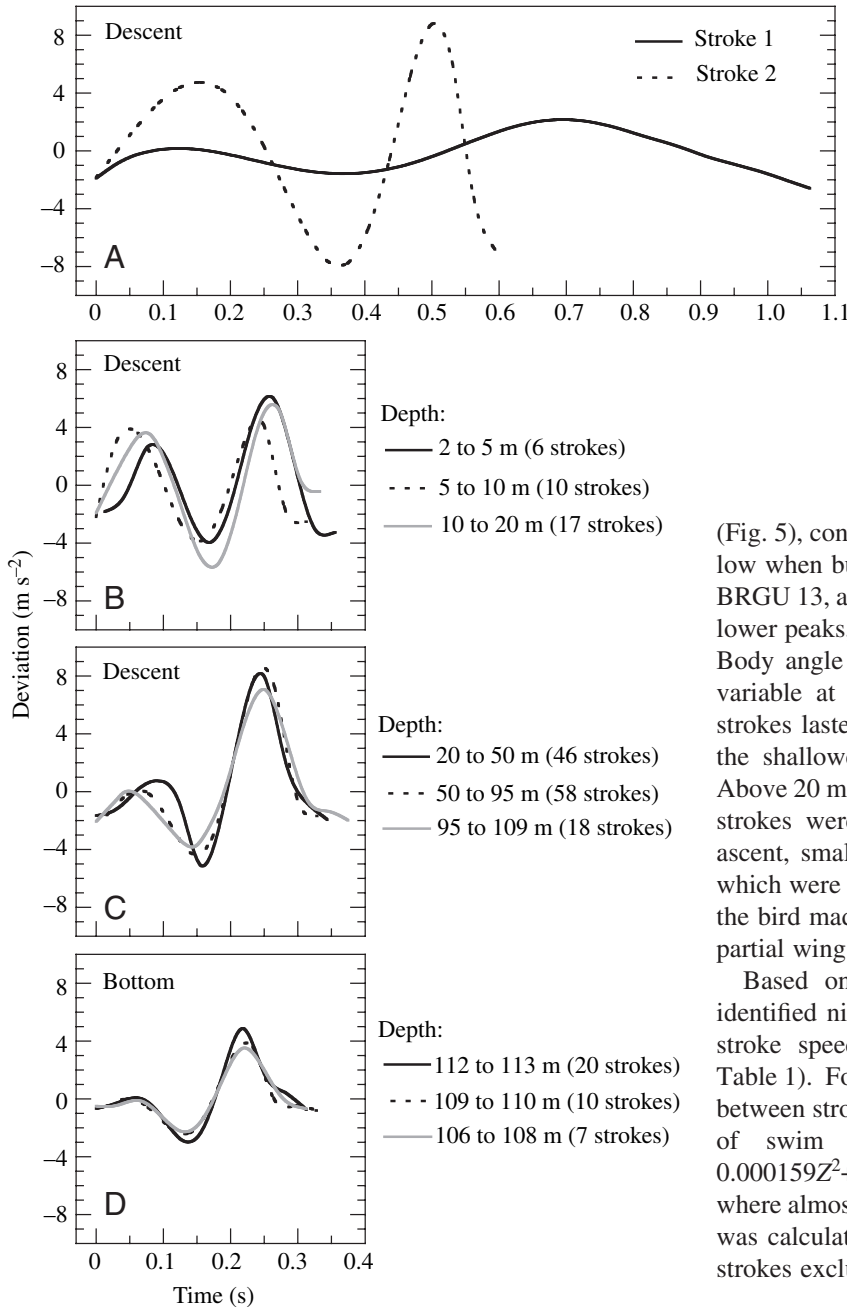


Fig. 4. Changes in acceleration parallel to the body fuselage (surge) throughout single swimming strokes by a Brunnich's guillemot (BRGU 13) during descent (A–C) and horizontal swimming at the bottom of a dive (D). Curves for depths >2 m during descent and at the bottom represent pooled groups of strokes with similar curves (numbers of pooled strokes in parentheses). Plots are of deviations from the mean acceleration during an entire stroke (including upstroke and downstroke), based on regression equations fitted to accelerometer recordings at 0.03125 s intervals (32 Hz). The first peak is for the upstroke, and the second for the downstroke. The first two entire strokes encompass a change in body angle from horizontal to vertical, perhaps confounding surge measurements.

(Fig. 5), consistent with the idea that relative upstroke thrust is low when buoyant resistance is low or negative. However, in BRGU 13, a few strokes from 71 to 61 m lasted longer and had lower peaks, resembling a single stroke that occurred at 42 m. Body angle was very constant below 60 m, becoming more variable at shallower depths (Fig. 3F). Above 50 m depth, strokes lasted much longer than below that depth, but within the shallower range, trends with depth were not apparent. Above 20 m where buoyancy increased dramatically (Fig. 3A), strokes were long and with little acceleration. Throughout ascent, smaller fluctuations in acceleration (peaks <1 m s⁻²), which were not clearly recognizable as strokes, suggested that the bird made minor adjustments to speed and body angle by partial wing movements without executing regular strokes.

Based on speed changes from acceleration curves, we identified nine basic curves standardized as fraction of mean stroke speed *v*_s fraction of stroke period (Figs 6 and 7, Table 1). For descent, where there was little or no gliding between strokes, mean speed was calculated from a regression of swim speed *U* vs depth *Z* ($U=1.193+0.0169Z-0.000159Z^2+4.877\times 10^{-7}Z^3$, $r^2=0.97$, $P<0.001$). For ascent, where almost all strokes were followed by gliding, mean speed was calculated separately for individual strokes or groups of strokes excluding glide periods. At the bottom, we calculated

Table 1. Regressions of fraction of mean speed during a stroke vs fraction of stroke period for a Brunnich's guillemot (BRGU 13), corresponding to the curves in Figs 6 and 7

Curve number	Equation
1	$F=0.9523+3.3535S-6.0476S^2-29.954S^3+56.275S^4-68.389S^8+120.05S^{11}-75.324S^{12}$
2	$F=0.7920+1.7457S+318.76S^5-1305.7S^6+4136.3S^8-12210S^{10}+13465S^{11}-4405.6S^{12}$
3	$F=0.9566-0.6284S+15.785S^2-51.741S^3+113.32S^5-286.65S^8+462.61S^{10}-252.70S^{11}$
4	$F=0.9973+7.2315S^2-62.263S^3+114.24S^4-642.01S^8+2668.3S^{10}-3199.1S^{11}+1113.6S^{12}$
5	$F=1.0105+2.1616S^2-23.344S^3+46.921S^4-484.96S^8+795.12S^9-634.93S^{11}+299.03S^{12}$
6	$F=0.6813+0.9324S-14.053S^3+21.635S^4+26.046S^6-391.73S^9+616.11S^{10}-258.41S^{11}$
7	$F=0.9676+0.0474S+0.3129S^2-8.1185S^4+247.97S^8-1449.5S^{10}+1991.5S^{11}-782.89S^{12}$
8	$F=0.9195+17.751S^2-57.290S^3+94.197S^5-257.48S^9+457.63S^{11}-254.87S^{12}$
9	$F=0.5753+0.8622S-0.8687S^2+42.819S^7-137.86S^9+210.35S^{11}-114.61S^{12}$

F, fraction of mean speed; *S*, fraction of stroke period.
For all regressions, $r^2>0.984$, $P<0.001$.

the fraction of stroke speed using a mean of 1.76 m s^{-1} , which was the descent speed at neutral buoyancy (71 m), and 2.18 m s^{-1} , which was the mean speed of COGU swimming horizontally in a tank 33.5 m long to reach food at the other end (Swennen and Duiven, 1991; see also Bridge, 2004). Resulting curves were about the same, so we pooled them to yield the curve for bottom swimming in Fig. 6. Although we did not include the first two strokes (Curves 1 and 2, Fig. 6) in calculations of dive cost, it is notable that speed was substantially greater on the upstroke than downstroke as the bird initially submerged and worked to overcome very high buoyancy at the start of the dive.

Patterns of work per stroke throughout dives

Based on estimated changes in buoyancy with depth (Fig. 3A), changes in speed throughout strokes for different stroke types (Fig. 6), and drag at those speeds (Fig. 1), a quasi-steady model was used to estimate mechanical work per stroke against drag, buoyancy, surge acceleration and all three combined throughout descent (Fig. 8). Costs of the first two strokes (Fig. 6) were not included. The importance of differences between stroke–acceleration patterns was evaluated by estimating costs if all strokes followed Curve 3 (actually occurring at depths of 2–20 m, Fig. 6), and if all strokes followed Curve 4 (actually occurring at depths >20 m). The importance of accounting for variations in speed throughout individual strokes was assessed by a third set of work curves that assumed steady speed, i.e. work against drag and buoyancy at the same mean speed without acceleration from oscillatory stroking. For drag, Curve 3 with similar thrust on upstroke and downstroke yielded almost the same work as the steady curve; Curve 4 with most thrust on the downstroke yielded slightly lower work against drag, but this effect was so small as to be negligible (Fig. 8). Differences among curves in work against buoyancy were also negligible. Inertial work to accelerate the body throughout single strokes (which did not include longer-term changes in mean speed among strokes) was slightly higher when thrust was more evenly distributed between upstroke and downstroke (Curve 3). Based on these differences among work components, the total cumulative work of descent was 6% higher for Curve 3 than Curve 4. Total cumulative work was 10% higher for Curve 3 and 4% higher for Curve 4 than when the costs of oscillatory stroking were not accounted for (steady curve, Fig. 8). Given that most of descent to 105 m (depths >20 m) would follow Curve 4 (Fig. 6), not considering stroke–acceleration patterns would cause underestimates of about 5–6% of total mechanical cost.

During ascent, work stroke^{-1} was consistent as the bird swam upward against negative buoyancy with a steady stroke pattern (Fig. 9). However, when near and above the depth of neutral buoyancy at about 71 m, increasingly variable stroke–acceleration patterns and stroke frequency resulted in

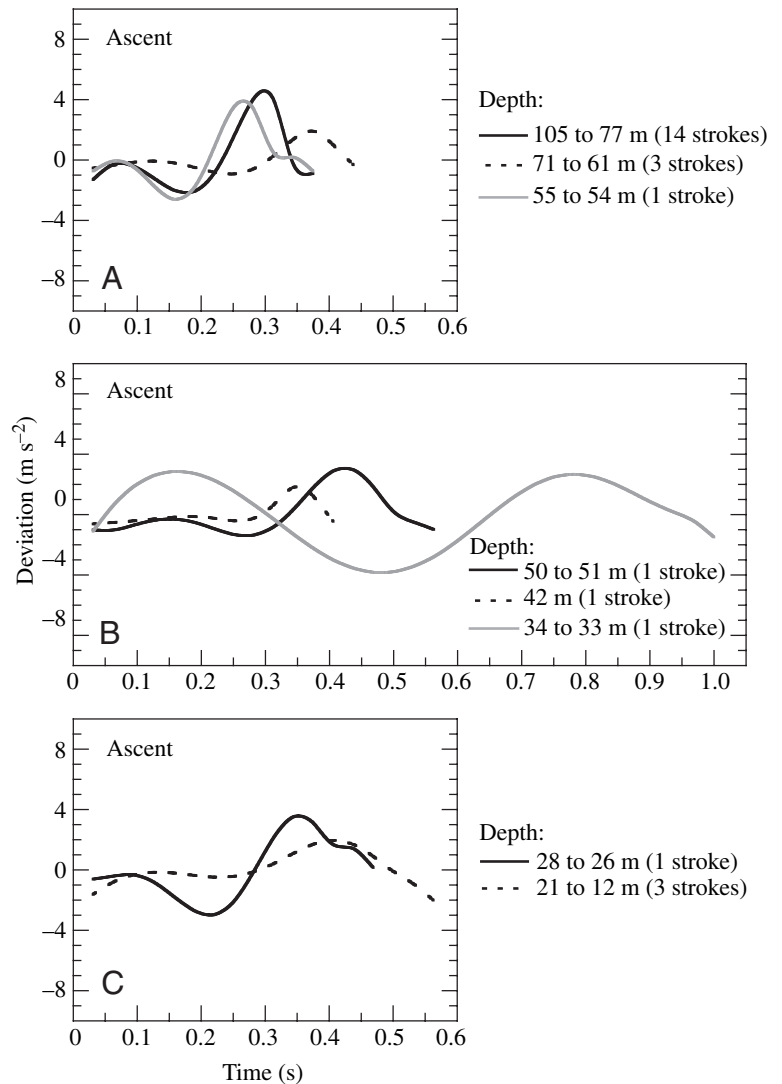


Fig. 5. Changes in acceleration parallel to the body fuselage (surge) throughout single swimming strokes by a Brünnich's guillemot (BRGU 13) during ascent. Plots are of deviations from the mean acceleration during an entire stroke (including upstroke and downstroke), based on regression equations fitted to accelerometer recordings at 0.03125 s intervals (32 Hz). Some curves represent pooled groups of strokes with similar curves (numbers of pooled strokes in parentheses). Periods of gliding separated almost all strokes, and only clearly recognizable strokes with acceleration peaks $>1 \text{ m s}^{-2}$ were included. Other conventions are as in Fig. 4.

highly variable work stroke^{-1} (note that work stroke^{-1} in Fig. 9 does not include intervening glide periods). Inertial work to accelerate the body fuselage based on Curve 7 (Fig. 7) at depths of 71–61 m and at 42 m was anomalously low (Fig. 9); apparently, the form of Curve 7 as derived from accelerometer data by our methods was incorrect or incomplete, perhaps due to changes in body angle. Glide periods separated each stroke during ascent, and these glides were fairly consistent in duration up to 80 m (Fig. 10). Above that depth, it was difficult to distinguish the ends of strokes from subsequent glide periods in the accelerometer data, because there was no discrete return of speed to that at the beginning of strokes (Fig. 7). Moreover,

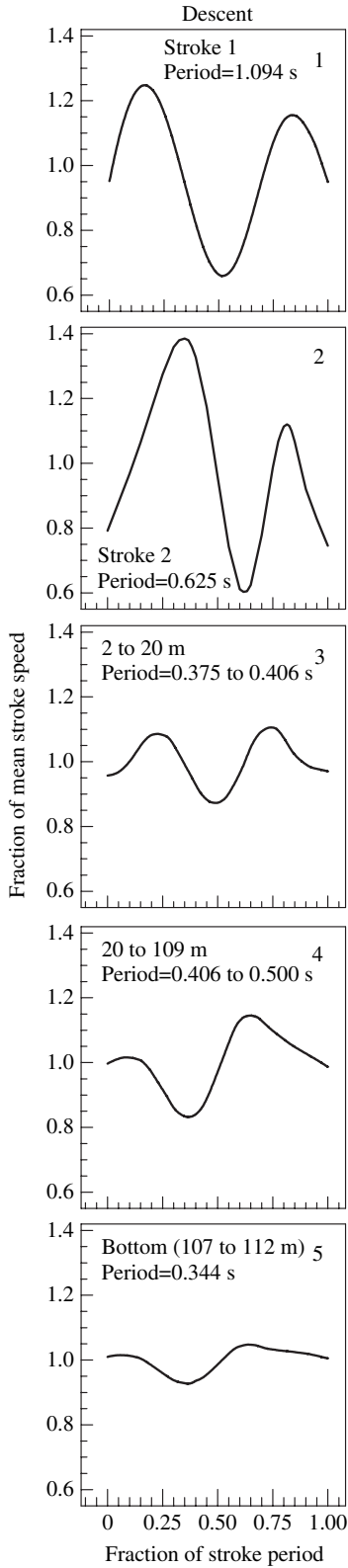


Fig. 6. Fraction of mean speed during a stroke vs fraction of stroke period (duration) corresponding to the five basic types of acceleration curve during descent and at the bottom in Fig. 4. At the bottom, curves were very similar when calculated for mean speeds of 1.76 and 2.18 m s⁻¹, and were subsequently pooled (see text). Equations for curves are in Table 1.

an increasing fraction of work against drag during ascent above 71 m was done passively by buoyancy (Fig. 3). Consequently, mechanical work stroke⁻¹ in Fig. 9 at depths shallower than 71 m is an unreliable measure of work done by the bird's muscles, and cannot be compared directly with work stroke⁻¹ during descent, horizontal swimming, or powered ascent from 105 to 80 m.

During descent (Fig. 8), total work stroke⁻¹ was highest in the first few meters, decreased to a low at 15–20 m, and then increased slightly to stabilize at 2.7 to 2.8 J stroke⁻¹ (Curve 4 for descent at >20 m). Work against drag and buoyancy were

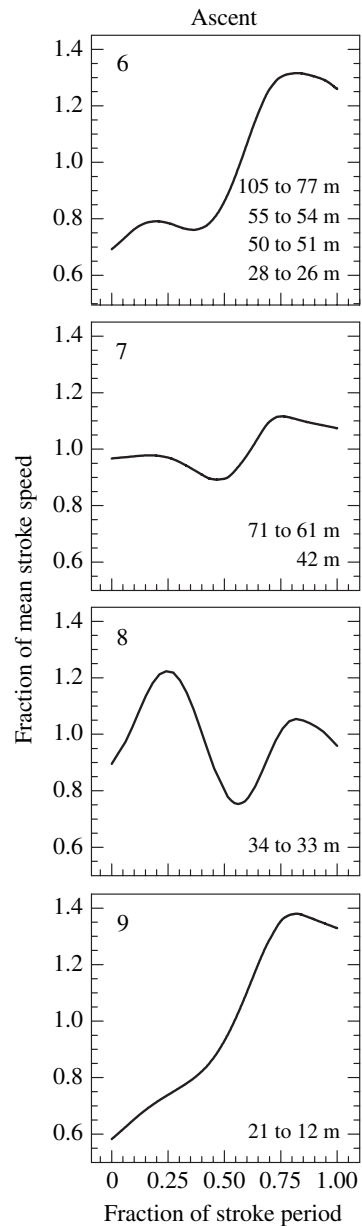
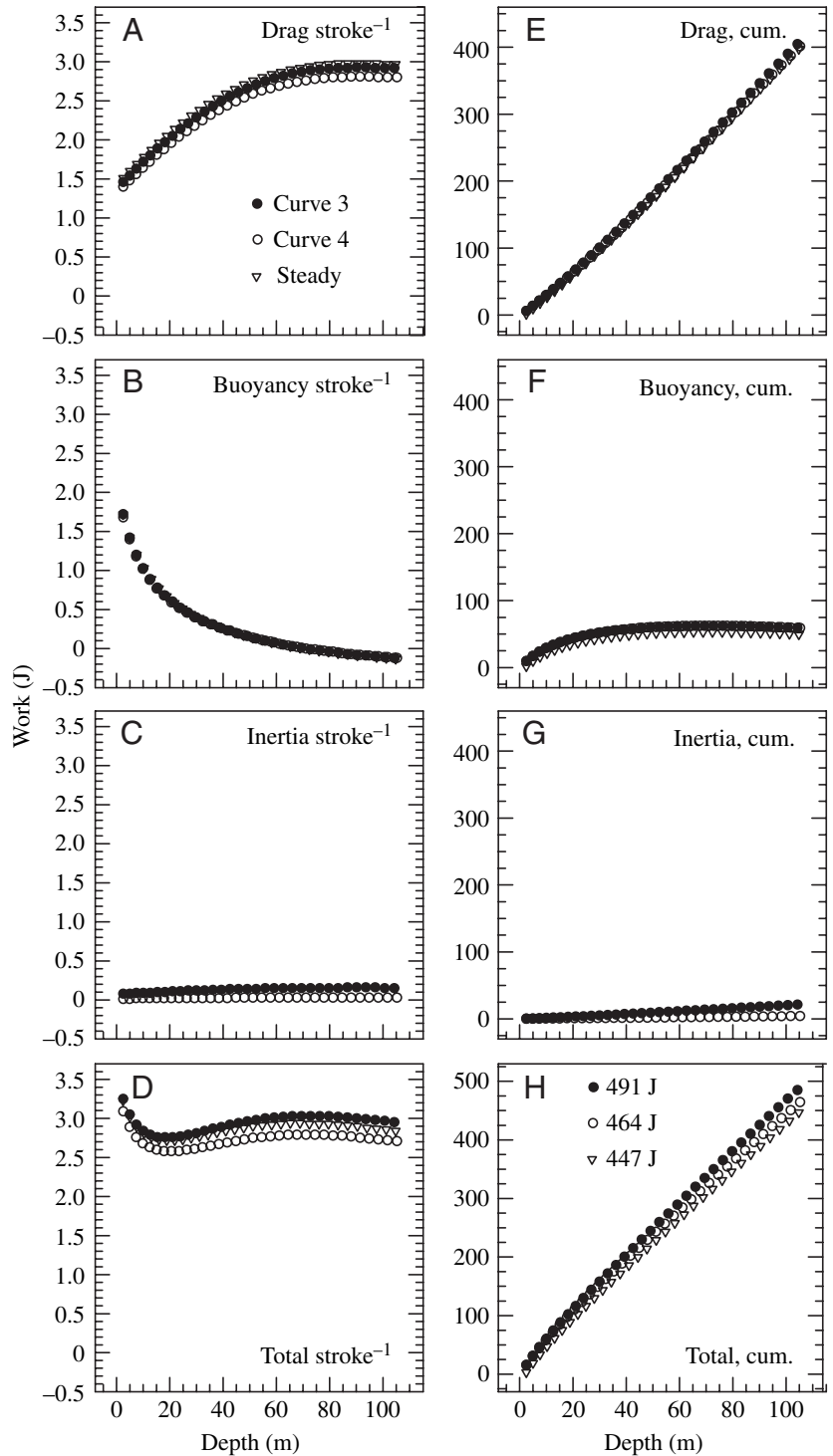


Fig. 7. Fraction of mean speed during a stroke vs fraction of stroke period (duration) corresponding to the four basic types of acceleration curve during ascent in Fig. 5. Equations for curves are in Table 1. Unlike curves for descent in Fig. 6, these curves did not have consistent periods and did not occur over particular depth ranges.

Fig. 8. Modeled changes in mechanical work stroke⁻¹ (A–D) and cumulative work (cum.; E–H) against drag (A,E), buoyancy (B,F), inertia (surge acceleration; C,G) and all three combined (D,H) during descent, based on dive parameters for a Brünnich's guillemot (BRGU 13; Figs 3 and 6; Table 1) and drag of a frozen Brünnich's guillemot (Fig. 1A). Solid circles are for a dive in which all strokes follow Curve 3 in Fig. 6, and open circles are for a dive in which all strokes follow Curve 4 in Fig. 6; triangles are for a dive in which the bird moves at steady speed with no oscillatory (accelerational) stroking. The total cumulative costs of descent for the three conditions are annotated in the bottom right panel. For work stroke⁻¹, very high values during the first (7.2 J) and second (5.2 J) strokes are not shown.



about the same initially, with buoyancy work decreasing rapidly with depth to become unimportant below 20 m, and drag increasing to become the main cost of descent (Fig. 8). Gradual increases in speed below 20 m (Fig. 3D) resulted in gradual increases in drag that roughly offset the gradual decline in buoyancy, so that total work stroke⁻¹ stayed about the same (Fig. 8). Additional simulations in which the volume of air in the respiratory system was varied over a likely maximum range ($\pm 60\%$) indicated that the resulting changes in buoyancy would result in variation of only $\pm 4.7\%$ in total mechanical cost of descent (Fig. 11).

Oscillatory stroking yielded small values of inertial work (Figs 8, 9), but affected drag by determining instantaneous speeds at which drag was exerted. During horizontal swimming at 109 m ('bottom', Fig. 9), work against buoyancy and inertia (acceleration) were negligible, with total work being attributed almost solely to drag. Total work per stroke at the bottom (2.4 J), based on an estimated mean speed of 1.76 m s^{-1} , was about 11% lower than during most of descent (2.7 J). During ascent, work per stroke was initially about the same as at the bottom (2.3 J), increasing to 3.3 J during the last strokes before reaching neutral buoyancy (Fig. 9). Thus, when strokes were discrete and recognizable, mechanical work per stroke varied between only 2.3 and 2.8 J throughout most of descent, bottom swimming, and initial (powered) ascent. Work against drag constituted almost all mechanical work during most of these strokes, and drag is a strong function of speed (Fig. 1). Thus, it appears that regulating speed serves to maintain work stroke⁻¹ within a relatively narrow range by regulating drag. Given this observation, can observed speed be predicted by identifying speeds that optimize drag?

Observed speeds of guillemots relative to drag

If work stroke⁻¹ by BRGU is calculated for a range of speeds at different depths during descent (Fig. 12), total work (essentially all against drag) rises slowly and almost linearly to a speed of about 2 m s^{-1} , rises at a slightly higher rate from 2 to 2.6 m s^{-1} , and then increases rapidly and nonlinearly at higher speeds. Note that effects of mean speed on drag are very similar for accelerational vs steady models (Fig. 8), so that

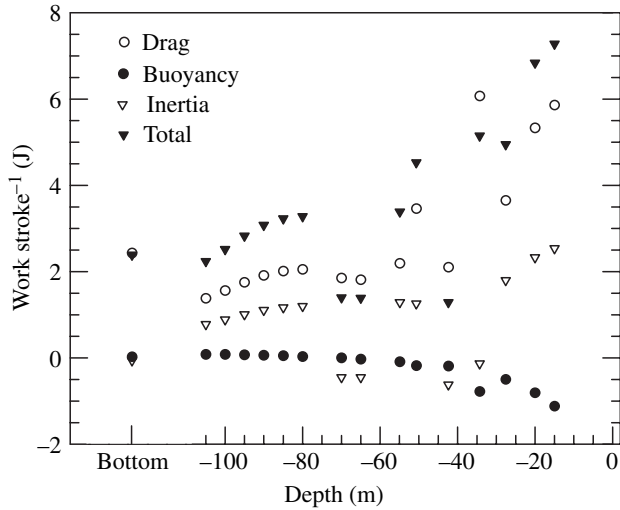


Fig. 9. Modeled changes in mechanical work stroke⁻¹ against drag, buoyancy, inertia (surge acceleration) and all three combined during ascent and horizontal swimming at the bottom (109 m), based on dive parameters for a Brünnich's guillemot (BRGU 13; Figs 3, 6 and 7; Table 1) and drag of a frozen Brünnich's guillemot (Fig. 1A). The depth of neutral buoyancy was estimated as 71 m (Fig. 3A). Values at the bottom were based on an estimated mean speed of 1.76 m s⁻¹.

effects of mean speed on total drag apply directly to costs of oscillatory stroking. In an earlier analysis based on the drag of a COGU mounted on a sting, it was concluded that observed speeds corresponded to a minimum in the curve of C_D vs Re (Fig. 1; see Lovvorn et al., 1999). $C_D:Re$ plots derived from a different measurement system, however, did not indicate this minimum (Fig. 1B). Free-ranging BRGU swam at speeds in the mostly linear part of the curve (less than about 2 m s⁻¹), before major increases in drag occur (Fig. 12). At speeds above the maximum of 2.6 m s⁻¹ observed in COGU swimming horizontally in a tank (Swennen and Duiven, 1991), rapid nonlinear increases in drag may impose a limit on achievable speeds.

Discussion

During descent and powered ascent to the depth of neutral buoyancy, Brünnich's guillemots (BRGU) maintained a mean swim speed of about 1.6 ± 0.2 m s⁻¹. Although thrust during the upstroke was almost as great as during the downstroke in the first 20 m of descent, most thrust was on the downstroke at greater depths during descent and horizontal swimming. However, these variations had minor effects (5–6%) on work stroke⁻¹ or cumulative work to propel the body fuselage, which did not include drag of the wings. For BRGU, these results suggest that mechanical costs of propelling the body fuselage can be modeled reasonably well without considering stroke–acceleration patterns, but only work against buoyancy and against drag at the mean swim speed. Even with substantial adjustments in respiratory air volume ($\pm 60\%$), modeled work against buoyancy was appreciable only in the top 15 m of

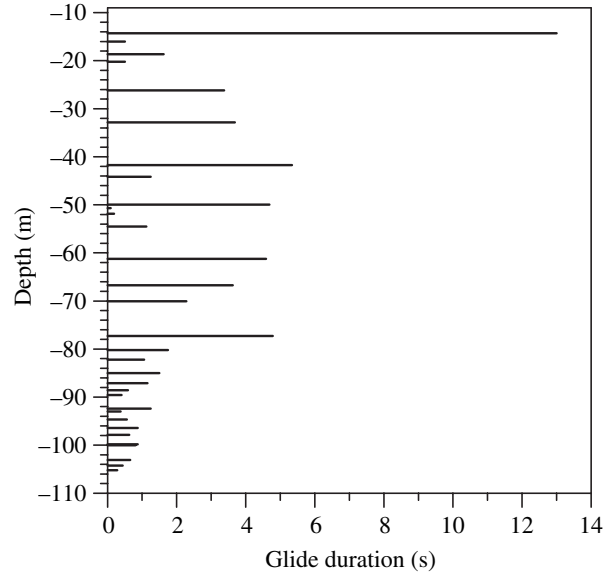


Fig. 10. Depth and duration of glides during a single ascent by a Brünnich's guillemot (BRGU 13). All glides were separated by a single stroke, except the glide at 44 m, which was preceded by two very short strokes in succession.

descent, after which almost all work was against drag. During descent below 10 m depth, small increases in speed and resulting drag offset gradual decreases in buoyancy, conserving work stroke⁻¹. Cruising speeds were well below maximum speed, which may be limited by rapid nonlinear increases in drag, or perhaps by maximum stroke frequency in this dense medium. During descent, there was little or no gliding between strokes, whereas all strokes during ascent were separated by gliding. During ascent above the depth of neutral buoyancy, stroke–acceleration patterns and work stroke⁻¹ were far more variable than during other dive phases. Nevertheless, the mean swim speed of guillemots during ascent was regulated within a relatively narrow range until buoyancy increased dramatically near the water surface.

Curves of drag vs speed and C_D vs Re

Curves of drag vs speed looked similar for tow-tank measurements on the same frozen specimen when either mounted on a sting or pulled with a harness and drogue system. However, small variations between the drag: speed curves resulted in appreciable differences between corresponding plots of C_D vs Re , with sting measurements indicating a much lower Re at which C_D was minimized (Fig. 1). This difference might have resulted from greater stability of the sting-mounted specimen at low speeds, but inability of the sting to adjust automatically to the angle of minimum drag at high speeds, as was possible with the harness and drogue (Lovvorn et al., 2001). Moreover, slight overestimates of drag at low speeds if the drag: speed data were fitted with quadratic or other low-order equations resulted in substantial overestimates of C_D at low Re , and thus an erroneous drop in C_D at higher Re . Consequently, to derive correct inference from the shape of

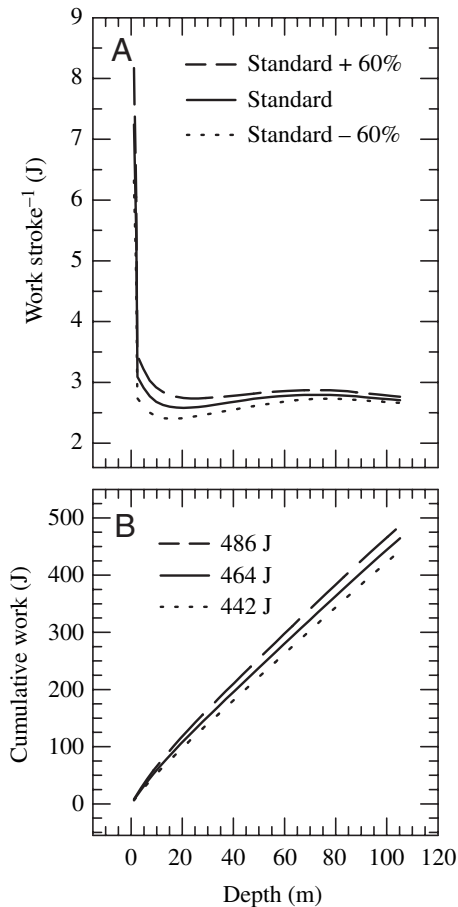


Fig. 11. Modeled changes in (A) total mechanical work stroke⁻¹ and (B) cumulative total work, throughout descent by a Brünnich's guillemot with the respiratory volume at the water surface assumed in all other simulations in this paper ('standard', 0.153 l), and with respiratory volume at the surface increased and decreased by 60%. Total mechanical work for entire dives is annotated in the lower figure.

$C_D:Re$ plots, the drag:speed curves from which they are calculated should be fit very closely (including multiple higher-order terms if needed) over the entire range of speeds.

Effects of buoyancy regulation

For sea turtles, marine mammals and penguins, it has been suggested that respiratory air volumes are manipulated to optimize buoyancy during dives to different depths, or else that dive depth or gliding behavior are adjusted to air volume and resulting buoyancy (Hustler, 1992; Skrovan et al., 1999; Minamikawa et al., 2000; Williams et al., 2000; Nowacek et al., 2001; Sato et al., 2002; Hays et al., 2004). However, for dives to >20 m by BRGU, substantial changes in air volume ($\pm 60\%$) had little effect on mechanical costs of descent (<5%, Fig. 11), and work against buoyancy was always negligible during horizontal swimming at the bottom at these depths (Fig. 9). As variations in respiratory volume may alter the depth at which penguins stop stroking during ascent (Sato et al., 2002), either the number of strokes or work stroke⁻¹ of

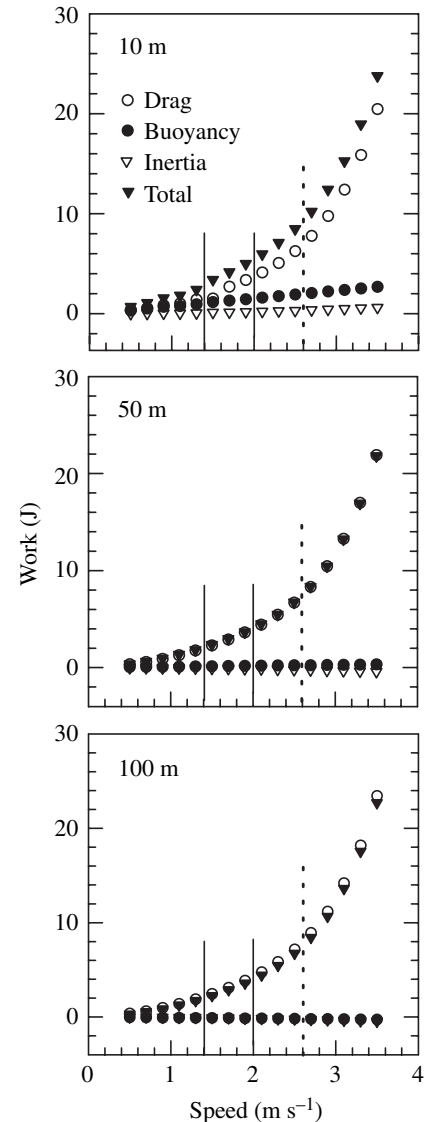


Fig. 12. Modeled changes in mechanical work stroke⁻¹ against drag, buoyancy, inertia (surge acceleration), and all three combined by a Brünnich's guillemot at a range of mean swim speeds during descent at depths of 10, 50 and 100 m. Vertical solid lines delimit the range of mean speeds observed in free-ranging Brünnich's guillemots (1.4–2 m s⁻¹, Figs 2 and 3). Vertical dotted line indicates the maximum speed observed in common guillemots swimming horizontally in a tank (about 2.6 m s⁻¹, Swennen and Duiven, 1991).

guillemots might still vary with respiratory adjustments during ascent.

Below about 40 m, however, changes in buoyancy with depth were quite small (Fig. 3A), as were buoyancy effects on the work of descent (Figs 8, 11). During the dive to 113 m by BRGU 13 (Fig. 3), only 6 of 25 strokes during ascent were above 40 m (Fig. 5). In comparison, there were 157 strokes during all of descent (Fig. 4), and at the bottom about 37 regular strokes and 2–3 times that many erratic strokes during pursuit of prey. Thus, the six strokes appreciably influenced by buoyancy during ascent would probably constitute at most 3% (for a bounce dive)

and typically less than 2% (for a foraging dive) of all strokes. Varying work during this 2–3% of strokes during ascent by a maximum $\pm 60\%$ through respiratory manipulation is unlikely to have an important influence on total dive costs. Consequently, although respiratory volume may secondarily affect the depth during ascent at which stroking ceases, effects on the energetics of diving *via* changes in buoyancy are probably minimal for deeper-diving species like BRGU. For diving depths typical of BRGU (Croll et al., 1992; Mehlum et al., 2001), effects of dive duration and intensity of prey pursuit on metabolic oxygen demand are probably the main considerations in any manipulation of respiratory air volume (Wilson, 2003).

Relative thrust on upstroke and downstroke

Before development of accelerometers that allowed direct measurements in free-ranging birds, stroke–acceleration patterns could be measured only by high-speed filming. Such filming is done during horizontal swimming or vertical dives in shallow tanks, where buoyancy is quite high and can strongly influence stroke–acceleration patterns (Hui, 1988; Lovvorn et al., 1991; Johansson and Aldrin, 2002; Johansson, 2003). Logger data from free-ranging guillemots showed that deceleration between upstroke and downstroke is much greater than in the hypothetical curves used previously in models for guillemots (Lovvorn et al., 1999). Moreover, the actual curves changed with depth (buoyancy) in ways undetectable in shallow tanks; in particular, much greater relative thrust on the upstroke was evident at depths <20 m during descent (Fig. 4).

Although large differences in relative upstroke thrust can theoretically have important effects on work stroke⁻¹ to propel the body fuselage (Lovvorn, 2001; Lovvorn and Liggins, 2002), variations directly measured on guillemots in this study had relatively small effects on simulated costs ($<6\%$). This difference resulted from the fact that the observed maximum fraction of mean stroke speed achieved during individual strokes (≤ 1.14 during descent, Fig. 6) was far less than for hypothetical curves used in previous models (≥ 1.6 ; Lovvorn et al., 1999; Lovvorn, 2001; Lovvorn and Liggins, 2002). Thus, even when the guillemots increased relative downstroke thrust, instantaneous speeds were still low enough to avoid rapid nonlinear increases in drag incurred by the hypothetical curves.

For birds and bats just after takeoff and during slow flight in air, downstroke lift and thrust predominate with little or no lift on the upstroke (Rayner et al., 1986; Hedrick et al., 2002; Spedding et al., 2003). Under such conditions, when lift is derived from generation of separate vortex rings shed at the end of each downstroke, lift must be imparted upward and not downward to support the bird's weight. Only after forward speed increases and lift is generated *via* a continuous-vortex wake does upstroke lift become important (Hedrick et al., 2002; Spedding et al., 2003). In contrast, penguins swimming horizontally underwater at shallow depths appeared to use downward lift during the upstroke to oppose buoyancy (Hui, 1988). The upstroke also imparted mainly a downward force on the body in Atlantic puffins *Fratercula arctica* swimming horizontally near the surface (Johansson, 2003).

During vertical descent, buoyancy directly opposes forward motion rather than being perpendicular to it, as is gravity during aerial flight or buoyancy during horizontal swimming. Consequently, in contrast to slow aerial flight when only the downstroke is suitable for overcoming gravity, both the upstroke and downstroke can generate useful lift and thrust for diving birds descending directly against high buoyancy. During the first two strokes of the dive (<2 m depth), thrust on the upstroke was substantially greater than on the downstroke (Fig. 6); e.g. in their first stroke, guillemots extend their wings under the water and sweep them upward as they pitch forward (J. R. Lovvorn, personal observation; Sanford and Harris, 1967). In the subsequent 2–20 m of the dive when the birds were increasing speed against appreciable buoyancy, they had similar thrust on upstroke and downstroke. Below that depth, where buoyancy was relatively unimportant and cruising speed had been achieved, thrust on the upstroke was much reduced. The latter pattern predominated throughout descent below 20 m, during sustained horizontal swimming at depths where buoyancy was negligible (Fig. 3), and during powered ascent to neutral buoyancy.

Therefore, it appears that the general pattern in air, in which takeoff and slow flight are dominated by the downstroke and the upstroke becomes important mainly in fast flight, is quite different from underwater flight during descent and during horizontal swimming at low buoyancy. For diving alcid, upstroke thrust appears to be important mainly when the opposing force is high, and perhaps during rapid acceleration while pursuing prey or escaping predators. Note that when the upstroke in Atlantic puffins was found to be appreciable (Johansson and Aldrin, 2002; Johansson, 2003), the birds were swimming horizontally near the surface, were stimulated to dive by approaching humans, and were filmed only 2–3 m from a standing start; thus, these birds were probably accelerating rather than swimming steadily, analogous to our guillemots swimming against high resistance in the first 20 m of descent. When swimming horizontally at lower buoyancy and more constant speeds, upstroke thrust was less apparent in our free-ranging birds. Hedrick et al. (2002) reported that birds in air increased *downstroke* thrust at very high speeds or when accelerating to high speeds, i.e. when flying directly against increasing drag forces. In contrast, guillemots swimming underwater appear to increase *upstroke* thrust when accelerating or swimming directly against high buoyancy.

Given that our BRGU did little or no gliding between strokes during descent, why was the upstroke thrust much reduced below 20 m? Dividing thrust equally between upstroke and downstroke resulted in about 6% higher work stroke⁻¹ in propelling the body fuselage (Fig. 8). It is likely that if drag of the wings were included in the model, their greater drag during a more active upstroke would have increased total work even more. For our free-ranging birds, we had no data on wing kinematics to calculate this effect. However, it appears that just as takeoff and slow flight without upstroke lift is more costly for aerial fliers than fast flight with upstroke lift (Marden, 1987; Ward et al., 2001), wing-propelled divers may face a similar

hurdle of less efficient but more powerful flight with strong upstroke to overcome initial high buoyancy and accelerate to cruising speed. After that, more efficient downstroke-based flight, perhaps with lower drag of the wings, is probably more viable (cf. Dial et al., 1997; Ward et al., 2001). Note that the relatively small effect of stroke–acceleration pattern on work to propel the body fuselage (Fig. 8) did not account for any differences in muscle efficiency or propulsive efficiency of the oscillating limbs. At any rate, it is clear that the relative function of upstroke and downstroke can vary greatly throughout dives, and that stroke–acceleration patterns measured with loggers on free-ranging birds provide critical insights to complement work in shallow tanks.

Why and how is speed regulated?

During sustained swimming, BRGU in this and similar studies (Lovvorn et al., 1999) maintained their speed at about $1.6 \pm 0.2 \text{ m s}^{-1}$, although COGU swimming horizontally in a tank could readily swim at $2.2\text{--}2.6 \text{ m s}^{-1}$ (Swennen and Duiven, 1991). Our free-ranging BRGU swam at speeds at the upper end of the mostly linear part of the drag curve, before major increases in drag occur (Fig. 12). However, there were no obvious thresholds of drag over this part of the curve to explain the observed range of cruising speeds. Above the maximum of 2.6 m s^{-1} observed for COGU, rapid nonlinear increases in drag may impose a limit on speeds achievable with available muscle power.

Swim speed might be limited by aerobic capacity of the muscles, whereby high speeds and associated high power output require unsustainable anaerobic metabolism (Dial et al., 1997; Pennycuik, 1997). In Atlantic puffins, fibers in muscles used for both upstroke and downstroke were mainly fast-twitch, highly oxidative, and only moderately glycolytic. However, the percentage of fast-twitch, moderately oxidative, highly glycolytic fibers in the main upstroke muscle (*supracoracoideus*) was higher (28%) than in the main downstroke muscle (*pectoralis*, 13%) (Kovacs and Meyers, 2000). This difference suggests that swimming with strong upstroke thrust as during early descent can involve greater anaerobic metabolism, perhaps discouraging use of the upstroke to achieve speeds beyond the usual range.

Several studies have suggested that marine mammals and birds regulate their swim speed by varying the duration of gliding between strokes (Skrovan et al., 1999; Williams et al., 2000; Watanuki et al., 2003). Before data on stroke frequency throughout dives were available, Lovvorn et al. (1999) suggested that guillemots maintain relatively constant work stroke⁻¹ to maximize muscle efficiency, while varying glide duration to modulate speed as buoyant resistance changes. Data from accelerometers in this study indicate that guillemots do indeed maintain relatively constant work stroke⁻¹, but make little use of gliding during descent. Because speed stays so similar despite large changes in buoyant resistance, guillemots may have regulated swim speed during descent by altering stroke amplitude or attack angle (see Zamparo et al., 2002), or by small decreases in stroke frequency (Fig. 3E), rather than gliding

between strokes. Variation in stroke amplitude as a means of modulating speed, alone or in addition to changes in stroke frequency, has recently been found in sea turtles, sea lions and penguins (Wilson and Liebsch, 2003).

For a range of penguin species during horizontal swimming, the duration of gliding generally increased with increasing body mass (1–30 kg; Clark and Bemis, 1979). Momentum to perpetuate a glide increases with body mass, and drag opposing the glide depends on surface area, which declines relative to body volume as mass increases. Respiratory air volume (and thus buoyant resistance to gliding during descent) also decreases allometrically with increasing body mass (see Materials and methods). Consequently, although they often glide during horizontal swimming, relatively small-bodied guillemots may be unable to glide as effectively during descent as do larger penguins and marine mammals.

Ascent with positive buoyancy

Stroke patterns during ascent from the bottom of the dive to the depth of neutral buoyancy (~71 m) were similar to those during descent and horizontal swimming; however, stroke–acceleration patterns and work stroke⁻¹ were different and quite variable during ascent with positive buoyancy. Despite maintaining relatively constant mean speed, the guillemot did not simply use the same stroke form with progressively longer glide periods as buoyancy increased during ascent (Figs 5, 7, 10). This unpredictable variation may have reflected searching the water column for prey that are more visible from below; however, the steady mean speed suggested no appreciable diversions to attack prey (cf. Ropert-Coudert et al., 2000; Wilson et al., 2002). Stroke–acceleration patterns might also have been confounded by irregular changes in body angle. Regardless of these variations and reasons for them, there were only 11 strokes from 71 m to the water surface during ascent, compared to 108 strokes during descent to 71 m. Thus, the error in estimating costs of strokes during ascent will have relatively small effects on estimates of the costs of travel to and from a prey patch.

Stroke patterns, cost and predicted speeds for diving birds

For deep-diving guillemots, variations in relative thrust on the upstroke vs downstroke had rather small effects on total dive costs (<6%). This pattern suggests that effects of drag on the body fuselage can be modeled reasonably well relative to mean speed without considering stroke–acceleration patterns. In smaller-bodied alcids, shearwaters and diving-petrels, which dive to shallower depths (Bocher et al., 2000), higher buoyancy, lower inertia and higher drag relative to body volume may increase effects of instantaneous speed during strokes. Such insights await further miniaturization of accelerometers. Stroke–acceleration patterns might also be more important for foot-propelled divers – with little positive thrust or even negative thrust during the recovery phase, swimming at the same mean speed requires higher instantaneous speeds during the power phase, perhaps incurring higher drag on the body fuselage (Lovvorn, 2001).

For guillemots, the maximum observed speed of about

2.6 m s⁻¹ (Swennen and Duiven, 1991) appears to correspond to the speed at which rapid nonlinear increase in drag begins (Fig. 12). The range of observed cruising speeds, with a mean about 1 m s⁻¹ below maximum speed, might correspond to optimal work against drag. However, there are no obvious breakpoints in the drag curve, making it difficult to predict optimum speeds based on that curve alone. Other factors such as the power output or efficiency of muscles for different speeds or stroking modes (e.g. Dial and Biewener, 1993; Dial et al., 1997) may determine optimal work against drag.

List of symbols and abbreviations

A_{sw}	wetted surface area
B	buoyancy
BRGU	Brünnich's guillemot
C_D	drag coefficient
COGU	common guillemot
COT	cost of transport
D	drag
F	fraction of mean speed
G	acceleration reaction
L_b	body length
M_a	added mass
M_b	body mass
Re	Reynolds number
S	fraction of stroke period
t	time
TDR	time-depth recorder
U	speed
V_b	total body volume
V_{plum}	volume of plumage air layer
V_{resp}	volume of air in the respiratory system
W	work
Z	water depth
α	added mass coefficient
ν	kinematic viscosity
ρ	density

We thank A. Akinturk and M. MacKinnon for help with drag measurements, S. M. Calisal for advice on drag measurements and for laboratory space, and G. W. Gabrielsen, Y. Niizuma and I. Nishiumi for field assistance. G. N. Stensgaard of the BC Research Ocean Engineering Center generously allowed use of the drag tank. We are especially grateful to G. V. Byrd, G. L. Hunt and A. L. SOWLS for collecting bird specimens. J.R.L. and G.A.L. were supported by US National Science Foundation, Office of Polar Programs grant OPP-9813979 to J.R.L., and a contract to J.R.L. from the Office of Ecological Services of the US Fish and Wildlife Service in Anchorage, Alaska. Y.W., A.K. and Y.N. were supported by Grant-in-Aid 04559014 from the Japanese Ministry of Education, Science and Culture, a Research Fellowship from the Japan Society for Promotion of Science, and the Sumitomo Foundation. The Norwegian Animal Research Authority and Governor of Svalbard permitted work on guillemots at Ny-Ålesund.

References

- Batchelor, G. K.** (1967). *An Introduction to Fluid Mechanics*. Cambridge: Cambridge University Press.
- Blake, R. W.** (1981). Influence of pectoral fin shape on thrust and drag in labriform locomotion. *J. Zool. Lond.* **194**, 53-66.
- Bocher, P., Labidoire, B. and Cherel, Y.** (2000). Maximum dive depths of common diving petrels (*Pelecanoides urinatrix*) during the annual cycle at Mayes Island, Kerguelen. *J. Zool. Lond.* **251**, 517-524.
- Boyd, I. L., Reid, K. and Bevan, R. M.** (1995). Swimming speed and allocation of time during the dive cycle in Antarctic fur seals. *Anim. Behav.* **50**, 769-784.
- Bridge, E. S.** (2004). The effects of intense wing molt on diving in alcids and potential influences on the evolution of molt patterns. *J. Exp. Biol.* **207**, 3003-3014.
- Clark, B. D. and Bemis, W.** (1979). Kinematics of swimming penguins at the Detroit Zoo. *J. Zool. Lond.* **188**, 411-428.
- Combes, S. A. and Daniel, T. L.** (2001). Shape, flapping and flexion: wing and fin design for forward flight. *J. Exp. Biol.* **204**, 2073-2085.
- Croll, D. A., Gaston, A. J., Burger, A. E. and Konnoff, D.** (1992). Foraging behavior and physiological adaptation for diving in thick-billed murre. *Ecology* **73**, 344-356.
- Culik, B. M., Wilson, R. P., Dannfeld, R., Adelung, D., Spairani, H. J. and Coco Coria, N. R.** (1991). Pygoscelid penguins in a swim canal. *Polar Biol.* **11**, 277-282.
- Daniel, T. L.** (1984). Unsteady aspects of aquatic locomotion. *Amer. Zool.* **24**, 121-134.
- Denny, M. W.** (1988). *Biology and the Mechanics of the Wave-swept Environment*. Princeton: Princeton University Press.
- Dial, K. P. and Biewener, A. A.** (1993). Pectoralis muscle force and power output during different modes of flight in pigeons (*Columba livia*). *J. Exp. Biol.* **176**, 31-54.
- Dial, K. P., Biewener, A. A., Tobalske, B. W. and Warrick, D. R.** (1997). Mechanical power output of bird flight. *Nature* **390**, 67-70.
- Dickinson, M. H.** (1996). Unsteady mechanisms of force generation in aquatic and aerial locomotion. *Amer. Zool.* **36**, 537-554.
- Dickinson, M. H., Lehmann, F.-O. and Sane, S. P.** (1999). Wing rotation and the aerodynamic basis of insect flight. *Science* **284**, 1954-1960.
- Fish, F. E.** (1988). Kinematics and estimated thrust production of swimming harp and ringed seals. *J. Exp. Biol.* **137**, 157-173.
- Fish, F. E.** (1993). Power output and propulsive efficiency of swimming bottlenose dolphins (*Tursiops truncatus*). *J. Exp. Biol.* **185**, 179-193.
- Gal, J. M. and Blake, R. W.** (1988). Biomechanics of frog swimming. II. Mechanics of the limb-beat cycle in *Hymenochirus boettgeri*. *J. Exp. Biol.* **138**, 413-429.
- Grémillet, D., Argentin, G., Schulte, B. and Culik, B. M.** (1998a). Flexible foraging techniques in breeding cormorants *Phalacrocorax carbo* and shags *Phalacrocorax aristotelis*: benthic or pelagic feeding? *Ibis* **140**, 113-119.
- Grémillet, D., Tuschy, I. and Kierspel, M.** (1998b). Body temperature and insulation in diving great cormorants and European shags. *Funct. Ecol.* **12**, 386-394.
- Grémillet, D., Wilson, R. P., Storch, S. and Gary, Y.** (1999). Three-dimensional space utilization by a marine predator. *Mar. Ecol. Prog. Ser.* **183**, 263-273.
- Hays, G. C., Metcalfe, J. D. and Walne, A. W.** (2004). The implications of lung-regulated buoyancy control for dive depth and duration. *Ecology* **85**, 1137-1145.
- Hedrick, T. L., Tobalske, B. W. and Biewener, A. A.** (2002). Estimates of circulation and gait change based on a three-dimensional kinematic analysis of flight in cockatiels (*Nymphicus hollandicus*) and ringed turtle-doves (*Streptopelia risoria*). *J. Exp. Biol.* **205**, 1389-1409.
- Hindell, M. A., Lea, M.-A., Morrice, M. G. and MacMahon, C. R.** (2000). Metabolic limits on dive duration and swimming speed in the southern elephant seal *Mirounga leonina*. *Physiol. Biochem. Zool.* **73**, 790-798.
- Houston, A. I. and Carbone, C.** (1992). The optimal allocation of time during the diving cycle. *Behav. Ecol.* **3**, 255-265.
- Hui, C. A.** (1988). Penguin swimming. I. Hydrodynamics. *Physiol. Zool.* **61**, 333-343.
- Hustler, K.** (1992). Buoyancy and its constraint on the underwater foraging behaviour of reed cormorants *Phalacrocorax africanus* and darters *Anhinga melanogaster*. *Ibis* **134**, 229-236.
- Johansson, L. C.** (2003). Indirect estimates of wing-propulsion forces in horizontally diving Atlantic puffins (*Fratercula arctica* L.). *Can. J. Zool.* **81**, 816-822.
- Johansson, L. C. and Aldrin, B. S. W.** (2002). Kinematics of diving Atlantic

- puffins (*Fratercula arctica* L.): evidence for an active upstroke. *J. Exp. Biol.* **205**, 371-378.
- Kochin, N. E., Kibel, I. A. and Roze, N. V.** (1964). *Theoretical Hydromechanics*. New York: Wiley.
- Kovacs, C. E. and Meyers, R. A.** (2000). Anatomy and histochemistry of flight muscles in a wing-propelled diving bird, the Atlantic puffin, *Fratercula arctica*. *J. Morphol.* **244**, 109-125.
- Lasiewski, R. C. and Calder, W. A.** (1971). A preliminary allometric analysis of respiratory variables in resting birds. *Respir. Physiol.* **11**, 152-166.
- Lighthill, M. J.** (1971). Large-amplitude elongated-body theory of fish locomotion. *Proc. R. Soc. Lond. B* **179**, 125-138.
- Lovvorn, J. R.** (2001). Upstroke thrust, drag effects, and stroke-glide cycles in wing-propelled swimming by birds. *Amer. Zool.* **41**, 154-165.
- Lovvorn, J. R. and Gillingham, M. P.** (1996). Food dispersion and foraging energetics: a mechanistic synthesis for field studies of avian benthivores. *Ecology* **77**, 435-451.
- Lovvorn, J. R. and Jones, D. R.** (1991a). Effects of body size, body fat, and change in pressure with depth on buoyancy and costs of diving in ducks (*Aythya* spp.). *Can. J. Zool.* **69**, 2879-2887.
- Lovvorn, J. R. and Jones, D. R.** (1991b). Body mass, volume, and buoyancy of some aquatic birds, and their relation to locomotor strategies. *Can. J. Zool.* **69**, 2888-2892.
- Lovvorn, J. R. and Liggins, G. A.** (2002). Interactions of body shape, body size and stroke-acceleration patterns in costs of underwater swimming by birds. *Funct. Ecol.* **16**, 106-112.
- Lovvorn, J. R., Jones, D. R. and Blake, R. W.** (1991). Mechanics of underwater locomotion in diving ducks: drag, buoyancy and acceleration in a size gradient of species. *J. Exp. Biol.* **159**, 89-108.
- Lovvorn, J. R., Croll, D. A. and Liggins, G. A.** (1999). Mechanical versus physiological determinants of swimming speeds in diving Brünnich's guillemots. *J. Exp. Biol.* **202**, 1741-1752.
- Lovvorn, J. R., Liggins, G. A., Borstad, M. H., Calisal, S. M. and Mikkelsen, J.** (2001). Hydrodynamic drag of diving birds: effects of body size, body shape and feathers at steady speeds. *J. Exp. Biol.* **204**, 1547-1557.
- Marden, J. H.** (1987). Maximum lift production during takeoff in flying animals. *J. Exp. Biol.* **130**, 235-258.
- Mehlum, F. and Gabrielsen, G. W.** (1993). The diet of high-arctic seabirds in coastal and ice-covered, pelagic areas near the Svalbard archipelago. *Polar Res.* **12**, 1-20.
- Mehlum, F., Watanuki, Y. and Takahashi, A.** (2001). Diving behaviour and foraging habitats of Brünnich's guillemots (*Uria lomvia*) breeding in the high-arctic. *J. Zool. Lond.* **255**, 413-423.
- Minamikawa, S., Naito, Y., Sato, K., Matsuzawa, Y., Bando, T. and Sakamoto, W.** (2000). Maintenance of neutral buoyancy by depth selection in the loggerhead turtle *Caretta caretta*. *J. Exp. Biol.* **203**, 2967-2975.
- Morison, J. R., O'Brien, M. P., Johnson, J. W. and Schaaf, S. A.** (1950). The force exerted by surface waves on piles. *Petrol. Trans. Amer. Inst. Mining, Metallurg. Petrol. Engin.* **189**, 149-157.
- Nowacek, D. P., Johnson, M. P., Tyack, P. L., Shorter, K. A. McLellan, W. A. and Pabst, D. A.** (2001). Buoyant balaenids: the ups and downs of buoyancy in right whales. *Proc. R. Soc. Lond.* **268**, 1811-1816.
- Pennycook, C. J.** (1997). Actual and 'optimum' flight speeds: field data reassessed. *J. Exp. Biol.* **200**, 2355-2361.
- Ponganis, P. J., Ponganis, E. P., Ponganis, K. V., Kooyman, G. L., Gentry, R. L. and Trillmich, F.** (1990). Swimming velocities in otariids. *Can. J. Zool.* **68**, 2105-2112.
- Rayner, J. M. V., Jones, G. and Thomas, A.** (1986). Vortex flow visualizations reveal change in upstroke function with flight speed in bats. *Nature* **321**, 162-164.
- Ropert-Coudert, Y., Sato, K., Kato, A., Charrassin, J.-B., Bost, C.-A., Le Maho, Y. and Naito, Y.** (2000). Preliminary investigations of prey pursuit and capture by king penguins at sea. *Polar Biosci.* **13**, 101-112.
- Ropert-Coudert, Y., Kato, A., Baudat, J., Bost, C.-A., Le Maho, Y. and Naito, Y.** (2001). Feeding strategies of free-ranging Adélie penguins *Pygoscelis adeliae* analysed by multiple data recording. *Polar Biol.* **24**, 460-466.
- Sanford, R. C. and Harris, S. W.** (1967). Feeding behavior and food-consumption rates of a captive California murre. *Condor* **69**, 298-302.
- Sarpkaya, T. and Isaacson, M.** (1981). *Mechanics of Wave Forces on Offshore Structures*. New York: Van Nostrand Reinhold.
- Sato, K., Naito, Y., Kato, A., Niizuma, Y., Watanuki, Y., Charrassin, J. B., Bost, C.-A., Handrich, Y. and Le Maho, Y.** (2002). Buoyancy and maximal diving depth in penguins: do they control inhaling air volume? *J. Exp. Biol.* **205**, 1189-1197.
- Skrovan, R. C., Williams, T. M., Berry, P. S., Moore, P. W. and Davis, R. W.** (1999). The diving physiology of bottlenose dolphins (*Tursiops truncatus*). II. Biomechanics and changes in buoyancy at depth. *J. Exp. Biol.* **202**, 2749-2761.
- Spedding, G. R.** (1992). The aerodynamics of flight. *Adv. Comp. Environ. Physiol.* **11**, 51-111.
- Spedding, G. R., Rosén, R. and Hedenström, A.** (2003). A family of vortex wakes generated by a thrush nightingale in free flight in a wind tunnel over its entire natural range of flight speeds. *J. Exp. Biol.* **206**, 2313-2344.
- Spring, L.** (1971). A comparison of functional and morphological adaptations in the common murre (*Uria aalge*) and thick-billed murre (*Uria lomvia*). *Condor* **73**, 1-27.
- Stephenson, R.** (1994). Diving energetics in lesser scaup (*Aythya affinis*, Eyton). *J. Exp. Biol.* **190**, 155-178.
- Swennen, C. and Duiven, P.** (1991). Diving speed and food-size selection in common guillemots, *Uria aalge*. *Neth. J. Sea Res.* **27**, 191-196.
- Thompson, D., Hiby, A. R. and Fedak, M. A.** (1993). How fast should I swim? Behavioural implications of diving physiology. *Symp. Zool. Soc. Lond.* **66**, 349-368.
- Tucker, V. A.** (1990). Body drag, feather drag and interference drag of the mounting strut in a peregrine falcon, *Falco peregrinus*. *J. Exp. Biol.* **149**, 449-468.
- van Dam, R. P., Ponganis, P. J., Ponganis, K. V., Levenson, D. H. and Marshall, G.** (2002). Stroke frequencies of emperor penguins diving under sea ice. *J. Exp. Biol.* **205**, 3769-3774.
- Ward, S., Möller, U., Rayner, J. M. V., Jackson, D. M., Bilo, D., Nachtigall, W. and Speakman, J. R.** (2001). Metabolic power, mechanical power and efficiency during wind tunnel flight by the European starling *Sturnus vulgaris*. *J. Exp. Biol.* **204**, 3311-3322.
- Watanuki, Y., Mehlum, F. and Takahashi, A.** (2001). Water temperature sampling by foraging Brünnich's guillemots with bird-borne data loggers. *J. Avian Biol.* **32**, 189-193.
- Watanuki, Y., Niizuma, Y., Gabrielsen, G. W., Sato, K. and Naito, Y.** (2003). Stroke and glide of wing-propelled divers: deep diving seabirds adjust surge frequency to buoyancy change with depth. *Proc. R. Soc. Lond. B* **270**, 483-488.
- Webb, P. W.** (1971). The swimming energetics of trout. I. Thrust and power output at cruising speeds. *J. Exp. Biol.* **55**, 489-520.
- Williams, T. M. and Kooyman, G. L.** (1985). Swimming performance and hydrodynamic characteristics of harbor seals *Phoca vitulina*. *Physiol. Zool.* **58**, 576-589.
- Williams, T. M., Friedl, W. A., Haun, J. E. and Chun, N. K.** (1993). Balancing power and speed in bottlenose dolphins (*Tursiops truncatus*). *Symp. Zool. Soc. Lond.* **66**, 383-394.
- Williams, T. M., Davis, R. W., Fuiman, L. A., Francis, J., Le Boeuf, B. J., Horning, M., Calambokidis, J. and Croll, D. A.** (2000). Sink or swim: strategies for cost-efficient diving by marine mammals. *Science* **288**, 133-136.
- Wilson, R. P.** (1991). The behaviour of diving birds. *Proc. Int. Ornithol. Congr.* **20**, 1853-1867.
- Wilson, R. P.** (2003). Penguins predict their performance. *Mar. Ecol. Prog. Ser.* **249**, 305-310.
- Wilson, R. P. and Liebsch, N.** (2003). Up-beat motion in swinging limbs: new insights into assessing movement in free-living aquatic vertebrates. *Mar. Biol.* **142**, 537-547.
- Wilson, R. P., Culik, B. M., Peters, G. and Bannasch, R.** (1996). Diving behaviour of Gentoo penguins, *Pygoscelis papua*; factors keeping dive profiles in shape. *Mar. Biol.* **126**, 153-162.
- Wilson, R. P., Hustler, K., Ryan, P. G., Burger, A. E. and Nöldeke, E. C.** (1992). Diving birds in cold water: do Archimedes and Boyle determine energetic costs? *Am. Nat.* **140**, 179-200.
- Wilson, R. P., Ropert-Coudert, Y. and Kato, A.** (2002). Rush and grab strategies in foraging marine endotherms: the case for haste in penguins. *Anim. Behav.* **63**, 85-95.
- Zamparo, P., Pendergast, D. R., Termin, B. and Minetti, A. E.** (2002). How fins affect the economy and efficiency of human swimming. *J. Exp. Biol.* **205**, 2665-2676.